The hybrid scale factor, the transition from the matter dominated era to the dark energy dominated era and time evolution of the Universe

Ekrem Aydiner (ekrem.aydiner@istanbul.edu.tr)
Istanbul University https://orcid.org/0000-0002-0385-9916
Isil Basaran-Oz
Istanbul University
Tekin Dereli
Koc University https://orcid.org/0000-0002-6244-6054
Mustafa Sarisaman
Istanbul University https://orcid.org/0000-0002-7148-0836

Research Article

Keywords: Cosmology, late time inflation, dark energy, dark matter, catastrophic transition

Posted Date: August 23rd, 2021

DOI: https://doi.org/10.21203/rs.3.rs-154304/v2

Version of Record: A version of this preprint was published at The European Physical Journal C on January 15th, 2022. See the published version at https://doi.org/10.1140/epjc/s10052-022-09996-2.

The hybrid scale factor, transition from the matter dominated era to the dark energy dominated era and time evolution of the Universe

E. Aydiner[1],* I. Basaran-Öz[1], T. Dereli[2],† and M. Sarisaman[1]
[1]*Department of Physics, Faculty of Science, İstanbul University 34134, Istanbul Turkey*
[2]*Department of Physics, Koç University, 34450 Sarıyer, İstanbul, Turkey*
(Dated: June, 2020)

The late time crossover from matter dominated era (represented power-law evolution) to the dark energy dominated era (represented exponential evolution) of the Universe evolution is the major problem in today's physical cosmology. Unless this critical transition problem is solved, it is not possible to reach a holistic theory of cosmology. To explain this critical transition we propose a new model where the dark matter and dark energy interacting through a potential. Based on the FLRW framework we analytically solve this model and obtain the scale factor $a(t)$. In addition, we numerically compute all cosmological quantities. We find more significant results to enlightening the physical mechanism of the critical transition.

Firstly, we show that the scale factor $a(t)$ has a hybrid form as $a(t) = a_0(t/t_0)^{\alpha}e^{ht/t_0}$. This is main and important result in the presented work, which clearly indicates that the transition from the power-law to the exponential expansion of the Universe. The numerical results clearly provide that there is a time crossover t_c in the scale factor a curve, which indicates the transition from the power-law to the exponential expansion of the Universe. Below $t/t_0 \leq t_c$, matter era dominated hence time evolution of the Universe is given by $a(t) \propto (t/t_0)^{\alpha}$, on the other hand, above $t/t_0 > t_c$, the evolution is represented by $a(t) \propto \exp(ht/t_0)$. It is first time, the hybrid result for scale factor is exactly obtained from the presented model without use any approximation.

Secondly, we fit the scale factor below and above t_c. Surprisingly, we find that the scale factor behaves as $a(t) \propto (t/t_0)^{2/3}$ below $t/t_0 \leq t_c$, and as $a(t) \propto \exp(ht/t_0)$ which indicates that the Hubble parameter takes the value in the interval of the around $H_0 = 69.5$ and $H_0 = 73.5$ km s^{-1}Mpc^{-1} depend on the weak and strong interactions between dark components above $t/t_0 > t_c$, respectively. These are remarkable that $\alpha = 2/3$ is completely consistent exact solution of the FLRW and re-scaled Hubble parameter H_0 is the observable intervals given by Planck, CMB and SNIa data (or other combinations) for chosen interaction values are purely consistent with cosmological observations.

Thirdly, we find from the model the transition point from matter dominated era to the dark energy dominated era in the cosmic time is the $t_0 = 9.8$ Gyear which is consistent with the theoretical solution and observations.

Additionally, we numerically obtain and analyse other cosmological quantities such as dimensionless Hubble parameter h, deceleration parameter q, jerk parameter j and EoS parameter w. We show that all cosmological quantities of this model are consistent observational results for the matter and dark energy dominated eras.

As a result, we consider late time crossover of the Universe, we propose an interacting dark matter and dark energy model, we show that this model can explain the late time crossover phenomena of the Universe and our solutions are very good consistent with theoretical and observational results. Finally, we state that this work makes essential steps towards solving a critical outstanding problem of the cosmology, and has a potential to creates a paradigm for future studies in this field. Furthermore, the model also sheds light on the interaction mechanism of dark matter and dark energy in the Universe.

PACS numbers: 98.80.-k, 95.36.+x, 95.35.+d
Keywords: Cosmology, late time inflation, dark energy, dark matter, catastrophic transition

I. INTRODUCTION

In 1998, the accelerated expansion of the Universe was conjectured by two groups based on observations of Type Ia Supernova (SN Ia) [1, 2]. After this important observational discovery, the physical origin or mechanism of the accelerated expansion of the Universe became the most important challenge in modern cosmology. It was unexpected that the Universe was expanding with acceleration. We know from the time-line of the Universe evolution that after early time inflation [3, 4] the Universe passes through periods of radiation and matter-dominated eras, respectively.

* ekrem.aydiner@istanbul.edu.tr
† tdereli@ku.edu.tr

It is well-known that the evolution of the scale factor takes the functional form of $a \propto t^{1/2}$ in the radiation-dominated era. Meanwhile, it is given as $a \propto t^{2/3}$ in the matter-dominated era in the FLRW metric. These parameters can be obtained by solving the Friedmann equations. It is noticed that the expansion of the Universe in both periods is represented by the power-laws. However, the supernova observations were surprisingly different and indicate that the Universe is expanding exponentially as $a \propto \exp(H_0 t)$. Thus, the physical origin of exponential expansion appears to be a big challenging problem of current physical cosmology. It is intriguing to see that people have tried to explain this period by introducing the cosmological constant Λ or dark energy (DE) in the FLRW framework. This period is commonly called as dark-energy-dominated era. The physical origin of dark energy still remains to be a mystery. People suggested many interesting models in the literature trying to explain the origin of dark energy such as quintessence [5], phantom [6], k-essence [7], tachyon [8], Chaplygin gas [9], holographic dark energy [10]. However, these models do not provide a satisfactory answer to the most major problem of the transition from a power-law to an exponential expansion. This time crossover is one of the important cosmology problems and is known as a late time transition. In fact, is the reason of this transition the existence of dark energy? Even if dark energy can be considered to be the cause of late time exponential expansion of the Universe, the existence of dark energy alone does not seem to be sufficient to explain this transition. Although numerous models have been proposed to explain this phenomenon, this transition still has not been explained consistently Refs.[11–21]. Without understanding this critical transition, it seems to be unlikely to proceed toward a comprehensive theory of cosmology.

Based on this motivation, in this study, we will focus on the solution of the late time transition of the Universe and propose a new model to solve this challenging problem of the cosmology. Before presenting the model, we would like to point out a few points. Firstly, we know that the scale factor is a quantity which characterizes the time-dependent expansion dynamics of the Universe. However, in the previous theoretical models, a generalized scale factor to characterize all phases of the Universe was not proposed or obtained. The other point is rather distinct from the first one where the key question is: Can we describe this critical transition as a phase transition or a catastrophic transition? If we view the problem in terms of the statistical mechanics of phase transitions, we can not say that it is a first or second-order phase transition. The turnover in the evolution process favors a catastrophic jump rather than a phase transition (Please see [22] for the catastrophic transitions). It is clear that the problem is more sophisticated, and requires an elaborate approach. Therefore, we may need new players to enlarge this discussion. Possible candidates are baryonic or non-baryonic dark matter (DM) and dark energy. Indeed, it was recently suggested that dark energy could be dynamic, evolving with time [23–26]. Because, we know that the dynamics of the realistic the Universe is described by an EoS parameter which behaves differently at different epochs. Clearly, one can state that a single fluid with a constant can not give rise to a realistic cosmic history. Therefore, a realistic the Universe model should be dominated by more ingredients which can be defined by different EoS parameters [27]. In such a model, the components interact and dominate the evolution of the Universe [28].

Indeed, it is shown in the literature that the interacting models have potential to solve many problems of the cosmology. For example, many interacting models have been used to solve the singularity and cosmic coincidence problems [29–52]. More recently, a different interaction model has been introduced by Aydiner in Ref. [28]. In his study, it has been shown that the interaction between matter, dark matter and dark energy has lead to the chaotic evolution of the Universe. It was seen that this model combined the big-bang model and the oscillatory the Universe models, as well as had the potential to solve many fundamental problems of cosmology such as singularity, the future of the Universe, the formation of the galaxies and large-scale organization of the Universe. However, the late time transition was not specifically discussed by Aydiner in Ref. [28] and others. These studies provide a possible solution to the late time transition of the Universe based on interactions between dark energy and dark matter. Therefore, our aim in this study is to discuss the late time transition of the Universe based on the interaction of dark matter and dark energy. Here, for simplicity, we define these components as the two different scalar fields in the theoretical framework of the FLRW metric. We consider the interaction between them and generalize the model based on the motivation in Ref. [53]. In this study, Dereli and Tucker describe classical models of gravitation interacting with scalar fields whose solutions involve degenerate metrics. They show that some of these solutions exhibit transitions from a Euclidean domain to a Lorentzian spacetime corresponding to a spatially flat Robertson-Walker cosmology. Inspired from this study, here, we generalized the interacting scalar fields model to the dark matter and dark energy interaction in a flat Robertson-Walker cosmology.

To discuss the time crossover between power-law and exponential expansion of the Universe evolution, we set a Lagrangian based on the FLRW metric with two scalar fields interacting by a potential term. We introduce a suitable and exactly solvable potential from an interacting model which includes higher-order terms having a potential of catastrophic behaviour in dynamical evolution. We analytically solve this model and obtain the scale factor. By using the presented model we show that it is possible to explain the mechanism of this time crossover in the late-time evolution of the Universe. Additionally, we obtain and discuss other cosmological parameters such as dimensionless Hubble h, dimensionless deceleration q, dimensionless equation of states (EoS) w and dimensionless jerk parameters j for this model.

In summary, we propose a new interacting model to explain time evolution of the Universe. We explicitly obtain a hybrid scale factor incorporating the power and exponential terms as $a = a_0(t/t_0)^\alpha e^{ht/t_0}$ from the presented model. We perfectly predict the transition time point from matter dominated era to the dark energy era by model [54]. Additionally, we show that the obtained results are very consistent with the theoretical results [55] and all cosmological observations such as CMB with Planck [56–58], CMB without Planck [59–61], No CMB, with BBN [62–64], Cepheids-SNIa [65–74], and other combinations given in Ref. [75] (and references in therein). Additionally, we show that all computed dimensionless cosmological parameters are also consistent with theoretical expectations and observational data.

The rest of the paper is organized as follows. In section II, we present the two-scalar cosmology model with Lagrangian in the FLRW framework, we obtain Lagrangian solutions and discuss the corresponding potential. In Section III, we obtain a new scale factor a from the numerical results. We show that this transitional behavior in the evolution can be explained as a catastrophic transition from power-law expanding to the late inflation phase of the Universe. In Section IV, we numerically obtain the other cosmological quantities and discuss the time dependent characteristic behaviors of them. In Section V, we discuss the limit behavior of all quantities. Finally, we present the conclusion and important remarks of this study in the last section.

II. INTERACTION BETWEEN DM AND DE

In this study, we propose that DM and DE can be represented by two different scalar fields for instance ϕ and σ, and they interacts with a potential. In this case, the action of minimally coupled scalar gravity for two-scalar fields is described by

$$S = \int d^4x\sqrt{-g}\left[\frac{R}{2\kappa} + \frac{1}{2}(\partial_\mu\phi\partial^\mu\phi + \partial_\mu\sigma\partial^\mu\sigma) - V(\phi,\sigma)\right], \tag{1}$$

where ϕ, $\sigma : \mathbb{R}^4 \to \mathbb{R}$ are scalar-valued C^∞ fields, V is the potential expressed as a function of the scalar fields, R is the Ricci scalar, and $\kappa = 8\pi G/c^4$ is a constant that we use the geometric unit system, i.e. $\kappa = 1$. Scalar fields are defined on a manifold with metric $\gamma_{ab}(\phi,\sigma)$ and action is invariant under the symmetries of the scalar fields.

Consider the FLRW metric expressing a homogeneous isotropic space-time metric given by

$$ds^2 = h_{\mu\nu}\, dx^\mu dx^\nu, \tag{2}$$

with the metric $h_{\mu\nu} = \mathrm{diag}(-1, a(t)I_3)$, $I_3 = \mathrm{diag}(1,1,1)$ is 3×3 identity matrix, $a(t) : \mathbb{R} \to \mathbb{R}$ is a differentiable function which is known as time-dependent scale factor. The Ricci scalar equipped with this space-time (2) is specified by

$$R = 6\left(\frac{\ddot{a}}{a} + \frac{\dot{a}^2}{a^2}\right) \tag{3}$$

where the dot denotes the derivative with respect to time. Now, the point-like Lagrangian for DM and DE interaction can be written as follow

$$\mathcal{L} = -3a\dot{a}^2 + \frac{a^3}{2}\left(\dot{\phi}^2 + \dot{\sigma}^2\right) - a^3V(\phi,\sigma)\ . \tag{4}$$

At this point, we can obtain analytical solution using the Lagrangian (4).

III. ANALYTICAL RESULTS

One can easily reveal the set of equations of motion by means of the dynamical variables $\{a, \phi, \sigma\}$ for the Lagrangian (4). These are obtained as

$$2\frac{\ddot{a}}{a} + \frac{\dot{a}^2}{a^2} + \frac{1}{2}(\dot{\phi}^2 + \dot{\sigma}^2) - V(\phi,\sigma) = 0, \tag{5a}$$

$$\ddot{\phi} + 3\frac{\dot{a}}{a}\dot{\phi} + \frac{\partial V(\phi,\sigma)}{\partial\phi} = 0, \tag{5b}$$

$$\ddot{\sigma} + 3\frac{\dot{a}}{a}\dot{\sigma} + \frac{\partial V(\phi,\sigma)}{\partial\sigma} = 0. \tag{5c}$$

Notice that once we impose the zero energy condition, the remaining equation necessary for this theory is obtained as follows

$$-3\frac{\dot{a}^2}{a^2}+\frac{1}{2}\left(\dot{\phi}^2+\dot{\sigma}^2\right)+V(\phi,\sigma)=0. \tag{6}$$

To solve the equations of motion in Eqs.(5) and (6) we need to determine an appropriate potential which correspond to the two oscillators and two anti-oscillators. In our study, we focus our attention on a specific potential characterized by

$$2\alpha^2(X_1^2-X_2^2+Y_1^2-Y_2^2)V(\phi,\sigma)=A_1X_1^2+A_2X_2^2+B_1Y_1^2+B_2Y_2^2+2k_1X_1Y_2-2k_2X_2Y_1 \tag{7}$$

where A_j, B_j and k_j $(j=1,2)$ are interaction parameters.

Based on our experiences we know that this potential linearizes the field equations to get the precise solutions. However, in order to see that this potential gives rise to the physically meaningful and stable solutions, we have to check the potential surface. Therefore, inspired by the mechanical analogy, we introduce the following transformations

$$X_1=a^{3/2}\cosh(\alpha\phi), \tag{8a}$$
$$X_2=a^{3/2}\sinh(\alpha\phi), \tag{8b}$$
$$Y_1=a^{3/2}\cosh(\alpha\sigma), \tag{8c}$$
$$Y_2=a^{3/2}\sinh(\alpha\sigma), \tag{8d}$$

where $\phi,\sigma\in[-\infty,\infty]$ and $a:\mathbb{R}\to\mathbb{R}^+$. By using these transformations, we can write the potential V which explicitly depends on the scalar fields ϕ and σ as

$$\begin{aligned}V(\phi,\sigma)=\frac{1}{2\alpha^2}[&A_1\cosh^2(\alpha\phi)+A_2\sinh^2(\alpha\phi)+B_1\cosh^2(\alpha\sigma)+B_2\sinh^2(\alpha\sigma)\\&+k_1\cosh(\alpha\phi)\sinh(\alpha\sigma)-k_2\cosh(\alpha\sigma)\sinh(\alpha\phi)]\end{aligned} \tag{9}$$

where the parameters are given for $\theta=\pi/4$ and $\psi=\pi/4$ as

$$A_1=\Lambda_1\cos^2\theta+\Lambda_4\sin^2\theta, \tag{10a}$$
$$A_2=\Lambda_2\cos^2\psi+\Lambda_3\sin^2\psi, \tag{10b}$$
$$B_1=\Lambda_2\sin^2\theta+\Lambda_3\cos^2\theta, \tag{10c}$$
$$B_2=\Lambda_1\sin^2\theta+\Lambda_4\cos^2\theta, \tag{10d}$$
$$k_1=(\Lambda_1-\Lambda_4)\sin\theta\cos^2\theta, \tag{10e}$$
$$k_2=(\Lambda_2-\Lambda_3)\sin\psi\cos^2\psi, \tag{10f}$$

where Λ_i $(i=1,..,4)$ are also interaction constants. Employing the coordinate transformation to Eq. (6) we can write the Hamiltonian constraint in the form

$$\dot{X}_1^2-\dot{X}_2^2+\dot{Y}_1^2-\dot{Y}_2^2-A_1X_1^2-A_2X_2^2-B_1Y_1^2-B_2Y_2^2-2k_1X_1Y_2+2k_2X_2Y_1=0. \tag{11}$$

From this equation, we find relation between parameters as $A_1\neq\pm B_2$, $A_3\neq\pm B_1$, $A_1+A_2=B_1+B_2$, $k_1=-1/2(A_1+B_2)$ and $k_2=-1/2(A_2+B_1)$. These relations satisfy Hamiltonian constraint equations.

On the other hand, here, for the sake of simplicity and analyse of the minima of the potential, we set $k_1=-k_2=k$. Then, the potential becomes

$$V(\phi,\sigma)=\frac{1}{2\alpha^2}\left[\delta_1+\delta_2\sinh^2(\alpha\phi)+\delta_3\sinh^2(\alpha\sigma)+2k\sinh[\alpha(\sigma-\phi)]\right] \tag{12}$$

where $\delta_1=(A_1+B_1)$, $\delta_2=(A_1+A_2)$, $\delta_3=(B_1+B_2)$ and $\alpha^2=3/4$. Furthermore, the potential $V(\phi,\sigma)$ should have natural identifications for small ϕ and σ. Therefore, we realize that the coefficients of $\phi^2/2$ and $\sigma^2/2$ terms can be identified by the positive-valued mass terms m_ϕ^2 and m_σ^2 respectively, and $V(0,0)$ by the cosmological constant Λ. Potential can be Taylor expanded up to the order of fifth terms as follows

$$\begin{aligned}V(\phi,\sigma)=&\frac{1}{2\alpha^2}(A_1+B_1)+\frac{k}{\alpha}(\sigma-\phi)+\frac{1}{2}(A_1+A_2)\phi^2+\frac{1}{2}(B_1+B_2)\sigma^2+\frac{k\alpha}{2}(\phi^2\sigma-\sigma^2\phi)\\&+\frac{k\alpha}{6}(\sigma^3-\phi^3)+\frac{k\alpha^3}{12}(\sigma^3\phi^2-\sigma^2\phi^3)+\mathcal{O}_6(\phi,\sigma),\end{aligned} \tag{13}$$

where $\mathcal{O}_6$ denotes the sixth and higher-order terms. We realize that this potential involves the associated potential terms in the catastrophic theory for small field variables.

In view of these results, the potential surface corresponding to V governed by the field variables ϕ and σ is displayed in Fig. 1. It is obvious that the potential surface has a global minimum in the limit of $k \to 0$ and $\nabla V(0,0) \to 0$. This minima guarantees that the solutions in Eq. (14) are stable.

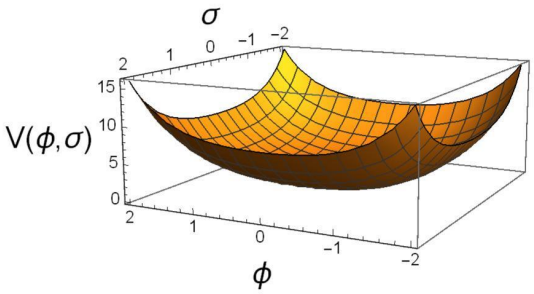

FIG. 1. The potential surface of V as a function of field variables ϕ and σ. We set values as $A_1 = B_2 = 1.005$, $A_2 = B_1 = 2.005$, $k = 0.005$.

The stable solutions arise around the minimal potential. These stable solutions also give rise to the stable cosmological solutions. Therefore, we see that in the limit of $k \to 0$, we get $\nabla V(0,0) \to 0$ for the appropriate parameter values. Based on this idea, the cosmological constant and the mass parameters of the scalar fields are obtained respectively as,

$$\Lambda := V(0,0) = \frac{2}{3}(A_1 + B_1), \tag{14a}$$

$$m_\phi^2 := \partial_\phi^2 V(0,0) = (A_1 + A_2), \tag{14b}$$

$$m_\sigma^2 := \partial_\sigma^2 V(0,0) = (B_1 + B_2). \tag{14c}$$

Using the expression in (7) and the transformations in (8), new Lagrangian can be written as

$$\mathcal{L} = \dot{X}_1^2 - \dot{X}_2^2 + \dot{Y}_1^2 - \dot{Y}_2^2 + A_1 X_1^2 + A_2 X_2^2 + B_1 Y_1^2 + B_2 Y_2^2 + 2k_1 X_1 Y_2 - 2k_2 X_2 Y_1. \tag{15}$$

Thus, by linearization, instead of non-linear field equations in (5), four linear field equations are obtained as follows

$$\ddot{X}_1 = A_1 X_1 + k_1 Y_2, \tag{16a}$$

$$\ddot{X}_2 = -A_2 X_2 + k_2 Y_1, \tag{16b}$$

$$\ddot{Y}_1 = B_1 Y_1 - k_2 X_2, \tag{16c}$$

$$\ddot{Y}_2 = -B_2 Y_2 - k_1 X_1 \ . \tag{16d}$$

These equations can be expressed in a more compact form with the identification

$$\xi = \begin{pmatrix} X_1 \\ X_2 \\ Y_1 \\ Y_2 \end{pmatrix} \tag{17}$$

such that (16) amounts to the following equation

$$\ddot{\xi} = \mathbb{M}\,\xi, \tag{18}$$

where $\mathbb{M}$ is the matrix obtained from the coefficients of field equations in (16). To find an appropriate solution of the Eq. (18), we first find out the eigenvalues and eigenvectors which are obtained by the characteristic equation $\det(\mathbb{M} - \lambda\mathbb{I}) = 0$. Thus, corresponding eigenvalues are attained as follows

$$\lambda_{1,2} = \frac{1}{2}\left[A_1 - B_2 \pm \sqrt{(A_1 + B_2)^2 - 4k_1^2}\right], \tag{19a}$$

$$\lambda_{3,4} = \frac{1}{2}\left[-A_2 + B_1 \pm \sqrt{(A_2 + B_1)^2 - 4k_2^2}\right], \tag{19b}$$

where we denote the distinct eigenvalues by means of "±" sign elements. The corresponding eigenvectors can be obtained accordingly

$$S_1(\lambda_i) = B_2 + \sum_{i=1}^{4} \lambda_i - k_1, \tag{20a}$$

$$S_2(\lambda_i) = B_1 - \sum_{i=1}^{4} \lambda_i + k_2, \tag{20b}$$

$$S_3(\lambda_i) = A_2 + \sum_{i=1}^{4} \lambda_i + k_2, \tag{20c}$$

$$S_4(\lambda_i) = A_1 - \sum_{i=1}^{4} \lambda_i - k_1 \ . \tag{20d}$$

As a result, eigenvalues in Eq. (19) and eigenvectors in Eq. (20) give rise to the exact solutions of the field equations, which take the following form in components

$$\xi_i = \sum_{i,j} S_i(\lambda_j)(\alpha_j + \beta_j), \tag{21}$$

where $\alpha_j = m_j e^{\sqrt{\lambda_j}t}$, $\beta_j = n_j e^{-\sqrt{\lambda_j}t}$, m_j and n_j are constants and $i, j = 1, 2, 3, 4$. It is to be not that here t is assumed as dimensionless parameter.

In view of these findings, we now return to our main discussion to find the solutions of cosmological quantities. At this point, we can give solutions to cosmological quantities for the Lagrangian in Eq. (4) with two scalar fields. In fact, the basic cosmological parameter is the scale factor a that is completely independent of position or direction and tells us how the expansion or contraction of the Universe depends on the cosmic time. We can present the scalar factor $a(t)$ in terms of the new coordinate variables as

$$a(t) = \left[\frac{1}{2}(\xi_1^2 - \xi_2^2 + \xi_3^2 - \xi_4^2)\right]^{\frac{1}{3}} \ . \tag{22}$$

On the other hand, the scalar fields ϕ and σ that appear in the Lagrangian which represent dark matter and dark energy, respectively, are given in the form:

$$\phi(t) = \frac{1}{\alpha} \tanh^{-1}\left(\frac{\xi_2}{\xi_1}\right), \quad \sigma(t) = \frac{1}{\alpha} \tanh^{-1}\left(\frac{\xi_4}{\xi_3}\right) . \tag{23}$$

Other cosmological parameters such as dimensionless Hubble h, deceleration q and jerk j parameters can be expressed in terms of a, $\dot{a}$, $\ddot{a}$ and $\dddot{a}$ as follows

$$H := \frac{\dot{a}}{a}, \quad q := -\frac{\ddot{a}}{aH^2}, \quad j := \frac{\dddot{a}}{aH^3} \ . \tag{24}$$

These parameters can be determined from Taylor's expansion of the scale factor a. Here, by definition, the Hubble parameter H tells us the cosmic time-dependent expansion rate of the Universe, the Deceleration parameter q tells us the change in the expansion rate of the Universe and the Jerk parameter j tells us the change in the acceleration or deceleration of the Universe. Additionally, the effective equation of state (EoS) parameter is given in terms of the effective pressure p_{eff} and effective density ρ_{eff} as follows

$$w_{eff} = \frac{p_{eff}}{\rho_{eff}}, \tag{25}$$

where the pressure is given by the expression $p_{eff} = \frac{1}{2}\dot{\phi}^2 + \frac{1}{2}\dot{\sigma}^2 - V(\phi, \sigma)$, whereas the density is provided by $\rho_{eff} = \frac{1}{2}\dot{\phi}^2 + \frac{1}{2}\dot{\sigma}^2 + V(\phi, \sigma)$.

IV. NUMERICAL RESULTS OF THE SCALE FACTOR

We solve field equations in Eq. (16) and analytically obtain the scale factor $a(t)$ in Eq. (22). Now, we give the numerical result of the scale factor in Fig. 2 for relatively weak and relatively strong interactions. In this numerical

solutions, we set parameters arbitrarily as $\Lambda_1 = 0.05$, $\Lambda_2 = 2.5$, $\Lambda_3 = 0.5$, $\Lambda_4 = 2.05$, $A_1 = A_4 = 1.05$, $A_2 = A_3 = 1.5$, $k_1 = -1.0$, $k_2 = 1.0$ for the red circle line; $\Lambda_1 = 0.1$, $\Lambda_2 = 2.6$, $\Lambda_3 = 0.6$, $\Lambda_4 = 2.2$, $A_1 = A_4 = 1.15$, $A_2 = A_3 = 1.6$, $k_1 = -1.05$, $k_2 = 1.0$ for the green star line, where here and in what follows, these parameters are selected such that minimal and stable potential together with minimal/maximal interactions for small/large k values are guaranteed.

The numerical solution of the dimensionless scale factor in Eq. (22) versus scaled axes t/t_0 is given in Fig. 2(a). However, the dimensionless scale factor is provided by log-log and semi-log scale in Fig. 2(b) and (c), respectively. When we fit the data of the dimensionless scale factor in Fig. 2(a) we see that our data give a hybrid relation as

$$a(t) = \left[\frac{1}{2}(\xi_1^2 - \xi_2^2 + \xi_1^2 - \xi_2^2)\right]^{\frac{1}{3}} = a_0 \left(\frac{t}{t_0}\right)^{\alpha} e^{h\frac{t}{t_0}} \ . \tag{26}$$

where little h is the dimensionless Hubble parameter [54, 76, 77] and t_0 is a constant. It first time, we precisely obtain a hybrid scale factor by using an interacting model. This is very interesting and amazing result. We show that an scale factor cover, at the same time, the power-law and exponential behavior without using any approximation or ansatz. Furthermore, this result provide that our model can explain the time evolution of the matter dominate era and dark energy dominated era. On the other hand, to obtain detail results and to determine parameter of the scale factor in Eq. (26) we plot log-log and semi-log of this quantity in n Figs. 2(b) and (c). It can be observed from the log-log plot in Fig. 2(b) that the scale factor increases by a power-law up to a crossover time t_c point. On the other hand, above this critical point, it increases exponentially as seen in Fig. 2(c). This crossover point indicates the transition from power-law expansion to the exponentially expanding era of the Universe. This extraordinarily important and surprising result solves the late-time transition problem which is one of the most important problems of cosmology. Our numerical results clearly show that the transition in the scale factor $a(t)$ can be represented by

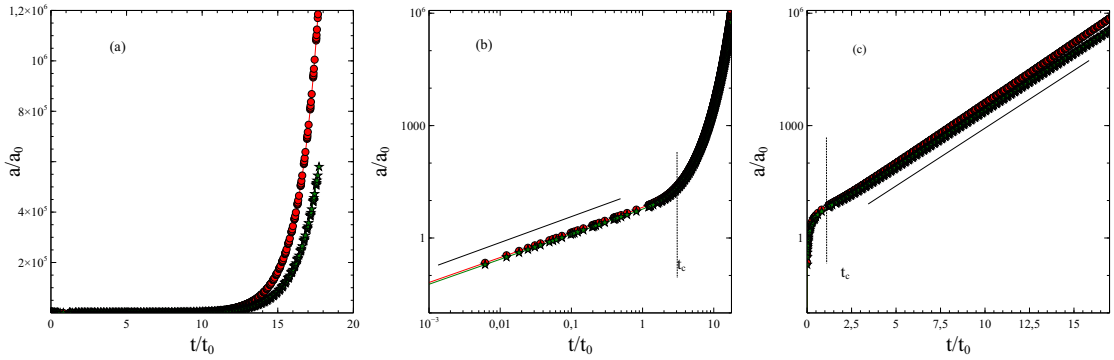

FIG. 2. In (a), the scale factor $a(t)$ with respect to the cosmic time is given. Here we set the parameter values $\Lambda_1 = 0.05$, $\Lambda_2 = 2.5$, $\Lambda_3 = 0.5$, $\Lambda_4 = 2.05$, $A_1 = A_4 = 1.05$, $A_2 = A_3 = 1.5$, $k_1 = -1.0$, $k_2 = 1.0$ for the red circle line; $\Lambda_1 = 0.1$, $\Lambda_2 = 2.6$, $\Lambda_3 = 0.6$, $\Lambda_4 = 2.2$, $A_1 = A_4 = 1.15$, $A_2 = A_3 = 1.6$, $k_1 = -1.05$, $k_2 = 1.0$ for the green star line. In (b), scale factor in Log-Log scale is given. In (c), scale factor $a(t)$ in semi-log plot is displayed. Here t_c value is given by Eq. (28).

$$a(t) \propto \begin{cases} (t/t_0)^{\alpha} & \text{for} \quad t/t_0 \leq t_c, \\ e^{h(t/t_0)} & \text{for} \quad t/t_0 > t_c, \end{cases} \tag{27}$$

where t_c is also dimensionless parameter. We will discuss the t_c below.

We numerically solved Eq. (22) for various interacting parameters, and, interestingly we found power-law exponent as $\alpha = 2/3$ which is consistent with the Einstein-de Sitter solution of the Friedman equations for the matter dominated era. It is very consistent with the theoretical solutions [55]. This result denotes that matter dominated era evaluates with time $(t/t_0)^{2/3}$ for the $t \leq t_c$. On the other hand, we solved Eq. (22) for various interacting parameters, and we find that time the second term dominates the solution of scale factor $a(t)$ for the $t/t_0 > t_c$ as seen from Fig. 2(c). For example, for different two data set we plot the Fig. 2 and, in our analyses, surprisingly, we find that the dimensionless scale factor takes value between $h = 0.695$ and $h = 0.735$ around depend on interactions parameters. It is know that the time dependent Hubble parameter is defined as $H_0 = 100h$ km s^{-1}Mpc^{-1} [54, 76, 77]. According this definition the time-dependent Hubble parameters correspond to $H_0 = 69.5$ and $H_0 = 73.5$ km s^{-1}Mpc^{-1} for $h = 0.695$ and $h = 0.735$, respectively. These theoretical results are completely agree with the observational results CMB with Planck [56–58], CMB without Planck [59–61], No CMB, with BBN [62–64],and Cepheids-SNIa [65–74]. It is assume that the current value in the late time inflation phase is about $H_0 = 70.88$ km s^{-1}Mpc^{-1} due to Planck and SNIa observations. In the numerical procedure, we used arbitrary parameter values and we see that choosing different parameter values

does not change the character of the solution in Eq. (26). However, we see that choosing arbitrary parameters change, particularly, the slope of Fig. 2(b) and (c). According to our findings, we show that we can explain the late time crossover from power-law to exponential expansion of the Universe by using the FLRW model including DM and DE interactions. Furthermore, we explicitly obtain a real scale factor involving power and exponential terms in a single formula from the model. We report these results for the first time by using a model-dependent study.

In this section, finally, we discuss the t_c and t_0. The crossover time t_c can be approximately estimated from Fig. 2(b) and (c) as between 1.3 and 1.5. However, we know that the crossover time is equal to $t_c = t/t_0$ and which can be precisely obtained by using the relation $t_c^{2/3} = e^{ht_c}$. Thus, t_c can be determined by the following equation

$$\frac{\ln t_c}{t_c} = \frac{3h}{2} \ . \tag{28}$$

For the dimensionless Hubble parameter $h \simeq 0.7$ and $t \simeq 14$ Gyear this relation gives $t_c \simeq 1.428$ Gyear which provides that the value of the t_0 is $t_0 = 1/H_0 = 9.8$ Gyear which refers to Einsetin-de Sitter solution [55] (See also Eq. (6.33) in Ref. [54]. This is another very important result of the model. Thus, the model we propose also predicts the transition from matter dominated era to the dark energy era perfectly with full precision.

V. NUMERICAL RESULTS OF OTHER KINEMATIC PARAMETERS

In this section, we numerically obtain the dimensionless kinetic parameters such as Hubble parameter h, the deceleration parameter q, The jerk parameter j and the EoS parameter for relatively weak and relatively strong interactions. All of these parameters can be obtained from the scale factor a we obtained. In these numerical solutions, we set parameters arbitrarily as $\Lambda_1 = 0.05$, $\Lambda_2 = 2.5$, $\Lambda_3 = 0.5$, $\Lambda_4 = 2.05$, $A_1 = A_4 = 1.05$, $A_2 = A_3 = 1.5$, $k_1 = -1.0$, $k_2 = 1.0$ for the red circle line; $\Lambda_1 = 0.1$, $\Lambda_2 = 2.6$, $\Lambda_3 = 0.6$, $\Lambda_4 = 2.2$, $A_1 = A_4 = 1.15$, $A_2 = A_3 = 1.6$, $k_1 = -1.05$, $k_2 = 1.0$ for the green star line in all figures below. Here, our aim is to show the detail analysing of the characterising behaviour of these quantities and to provide that results of the model are consistent with the observational data.

A. The dimensionless Hubble parameter h

The Hubble parameter is given by the ratio of the rate of change of the scale factor to the current value of the scale factor a, which reflects the characteristic rate of the expansion of the Universe. The Hubble parameter can be obtained by using observational data, which depends on the red-shift. It takes different values for the radiation-dominated era, the matter-dominated era and late time inflation. In our case, Hubble parameter is obtained from the model. The time dependence of the dimensionless Hubble parameter for the present model is provided in Fig. 3. The time-dependent behavior of the dimensionless Hubble parameter is displayed in Fig. 3(a). However, the Hubble parameter is given by log-log and semi-log scales in Figs. 3(b) and (c), respectively.

It is to be noticed that the Hubble parameter has an anomaly depending on the scale factor a. It starts from a maximum value and rapidly drops to a minimum value, and then reaches up to a maximum value with time. This minima corresponds to the critical transition time t_c observed in scale factor behavior. Clearly, we expect the dramatic change of the Hubble parameter in the case of the phase-like catastrophic transition from matter dominate era to dark energy dominate era. However, this minima additionally emphasizes that before the catastrophic transition, there occurs a short deceleration in the expansion of the Universe. This is a very interesting point from which its physical meaning and mechanism can be discussed profoundly. In order to see some more details of the evolution of the dimensionless Hubble parameter, one can analyze the Figs. 3(b) and (c) further. In Fig. 3(b), it is seen that the Hubble parameter decreases as $h \propto (t/t_0)^{-\tilde{\alpha}}$ up to the critical time point t_c. On the other hand, above t_c, it increases exponentially as $h \propto e^{\tilde{\alpha}'(t/t_0)}$ and it reaches up to a constant value, as observed, for relatively weak and relatively strong interactions, where $\tilde{\alpha}$, and $\tilde{\alpha}'$ denote arbitrary constant parameters. The constant value of the dimensionless Hubble parameter h for our interaction parameter set refers to $H_0 = 69.5$ and $H_0 = 73.5$ km s^{-1}Mpc^{-1} for $h = 0.695$ and $h = 0.735$, respectively as seen in Fig. 3. This numerical solution shows the characteristic behaviour of the dimensionless Hubble parameter h, at the same time it provides that our model produce quite consistent result with observational data for the different cosmological eras of the Universe. Furthermore, it denotes the presence of the an anomaly at around the transition from the matter dominated era to the dark energy dominated era.

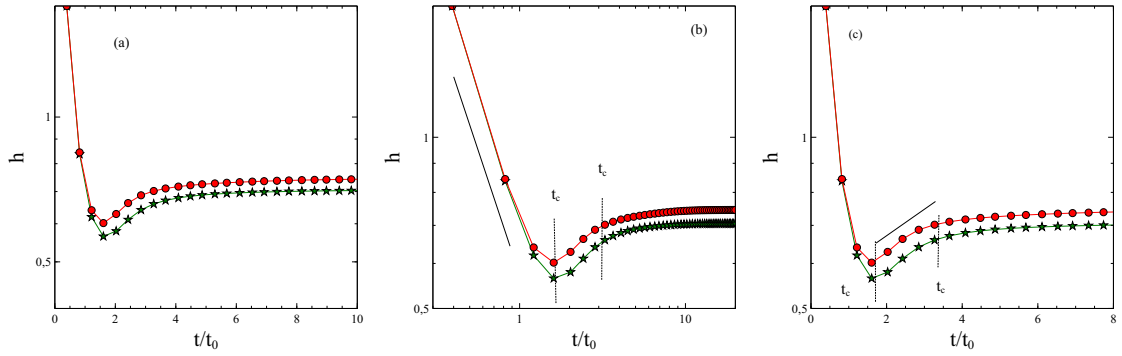

FIG. 3. In (a), the dimensionless Hubble parameter h with respect to cosmic time is given. Here we set the parameter values $\Lambda_1 = 0.05$, $\Lambda_2 = 2.5$, $\Lambda_3 = 0.5$, $\Lambda_4 = 2.05$, $A_1 = A_4 = 1.05$, $A_2 = A_3 = 1.5$, $k_1 = -1.0$, $k_2 = 1.0$ for the red circle line; $\Lambda_1 = 0.1$, $\Lambda_2 = 2.6$, $\Lambda_3 = 0.6$, $\Lambda_4 = 2.2$, $A_1 = A_4 = 1.15$, $A_2 = A_3 = 1.6$, $k_1 = -1.05$, $k_2 = 1.0$ for the green star line. In (b), Hubble parameter h in Log-Log scale is displayed. In (c), dimensionless Hubble parameter h in semi-log plot is shown.

B. The dimensionless deceleration parameter q

The deceleration parameter q in cosmology is a dimensionless measure of the cosmic acceleration of the expansion of space in a FLRW Universe. In general, q takes a negative sign and varies with the cosmic time, except in a few special cosmological models. Except in the speculative case of phantom energy, all postulated forms of mass-energy yield a deceleration parameter $q \geq -1$. On the other hand, for any non-phantom Universe, there must be a decreasing Hubble parameter, except in the case of the distant future of a ΛCDM model, where q goes to -1 from above and the Hubble parameter gets asymptote to a constant value of $H_0 \simeq \sqrt{\Lambda/3}$. In our case, the deceleration parameter is

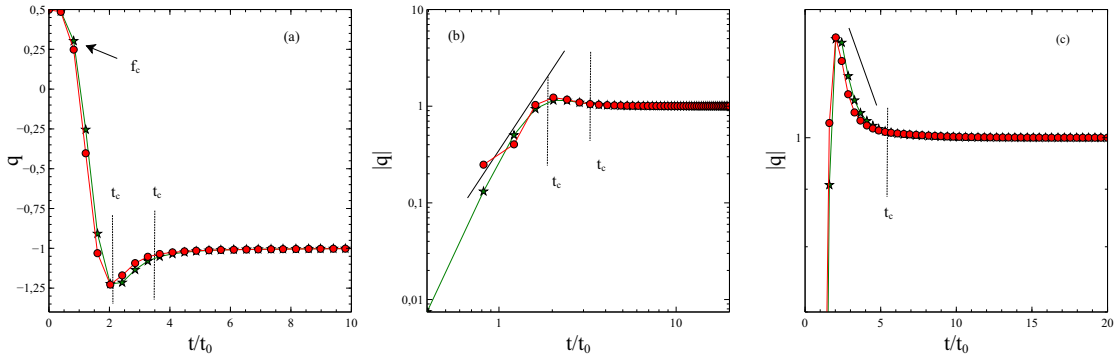

FIG. 4. The deceleration parameter q with respect to cosmic time is displayed. Here we set the parameter values $\Lambda_1 = 0.05$, $\Lambda_2 = 2.5$, $\Lambda_3 = 0.5$, $\Lambda_4 = 2.05$, $A_1 = A_4 = 1.05$, $A_2 = A_3 = 1.5$, $k_1 = -1.0$, $k_2 = 1.0$ for the red circle line; $\Lambda_1 = 0.1$, $\Lambda_2 = 2.6$, $\Lambda_3 = 0.6$, $\Lambda_4 = 2.2$, $A_1 = A_4 = 1.15$, $A_2 = A_3 = 1.6$, $k_1 = -1.05$, $k_2 = 1.0$ for the green star line. In (b), deceleration parameter q in Log-Log scale is shown. In (c), deceleration parameter q in semi-log plot is provided.

obtained from the model itself. The time dependence of the deceleration parameter for the present model is shown in Fig. 4. The time dependent behavior of the deceleration parameter is indicated in Fig. 4(a). However, the deceleration parameter is given by log-log and semi-log scale in Figs. 4(b) and (c), respectively. We note that log-log and semi-log figures are plotted for the absolute value of the deceleration parameter after first peaks f_c to yield the slope of the curves. Therefore, in Figs. 4(b) and (c), curves occur inversely.

As can be clearly seen that the sign of the phase-like transition also appears at the critical crossover time values t_c in Fig. 4(a). The deceleration parameter for the early time takes a positive value and rapidly drops to a minimum value at located t_c as seen from Fig. 4(a). In order to see some details of the time evolution of the deceleration parameter, one can see the Figs. 4(b) and (c). In Fig. 4(b), it is seen that the Hubble parameter decreases as $q \propto (t/t_0)^{-\tilde{\beta}}$ up to a critical time point t_c. On the other hand, after t_c, it increases exponentially as $h \propto e^{\tilde{\beta}'(t/t_0)}$ as seen in Fig. 4(c) and it reaches up to a constant value -1 with time for relatively weak and relatively strong interactions where $\tilde{\beta}$, and $\tilde{\beta}'$ denote arbitrary constant parameters.

C. The dimensionless jerk parameter j

In cosmology, the dimensionless jerk parameter j corresponds to the acceleration changes of expansion with respect to time. It is a very useful parameter to reveal the hidden transitions between phases of different cosmic accelerations. This parameter is defined as the dimensionless third derivative of the scale factor with respect to cosmic time. To confirm the presence of such a jump in the evolution of the expansion of the Universe, we carry out the presence of the phase-like catastrophic transition for our non-linear interacting two scalar fields model.

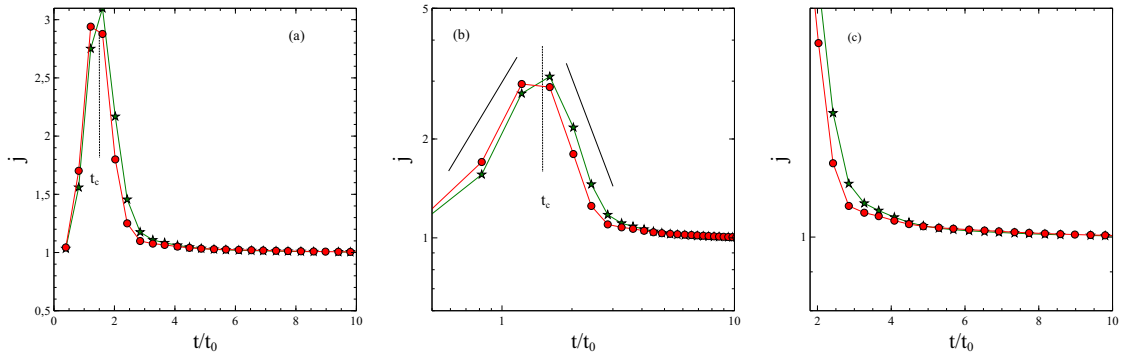

FIG. 5. The jerk parameter j with respect to cosmic time. Here we set the parameter values $\Lambda_1 = 0.05$, $\Lambda_2 = 2.5$, $\Lambda_3 = 0.5$, $\Lambda_4 = 2.05$, $A_1 = A_4 = 1.05$, $A_2 = A_3 = 1.5$, $k_1 = -1.0$, $k_2 = 1.0$ for the red circle line; $\Lambda_1 = 0.1$, $\Lambda_2 = 2.6$, $\Lambda_3 = 0.6$, $\Lambda_4 = 2.2$, $A_1 = A_4 = 1.15$, $A_2 = A_3 = 1.6$, $k_1 = -1.05$, $k_2 = 1.0$ for the green star line. In (b), jerk parameter j in Log-Log scale is provided. In (c), jerk parameter j in semi-log plot is shown.

The time dependence of the jerk parameter for the present model is displayed in Fig. 5. The time-dependent behavior of the jerk parameter is shown in Fig. 5(a). However, the jerk parameter is given by log-log and semi-log scale in Figs. 5(b) and (c), respectively. Notice that the peaks appear at critical crossover times. These cusps strongly indicate a transition in the time evolution of the scale factor a. In order to see some detailed time evolution of the jerk parameter around t_c, we give a log-log plot of the jerk parameter, as seen in Fig. 5(b). One can observe from this figure that the jerk parameter increases with a power-law exponent $j \propto (t/t_0)^{-\tilde{\gamma}}$ up to critical time point t_c and it decays with $j \propto (t/t_0)^{-\tilde{\gamma}'}$ where γ, and $\tilde{\gamma}'$ denote arbitrary constant parameters. Finally, after a local minimum value, by decreasing a very weak exponential with time, this parameter reaches up a constant value $j \to 1$ as well in the ΛCDM model as seen Fig. 5(c).

D. The dimensionless EoS parameter w

Finally, we study the EoS parameter w as a kinematic variable. The equation of state of a perfect fluid is characterized by a dimensionless number w, which is equal to the ratio of its pressure p to its energy density ρ. The equation of state may be used in FLRW equations to describe the evolution of an isotropic Universe filled with a perfect fluid. Cosmic inflation and the accelerated expansion of the Universe can be characterized by the equation of state of dark energy and it takes different values for different cosmic eras. In the simplest case, the equation of state of the cosmological constant is $w = -1$. In this case, the scale factor is given by $a \sim \exp(H_0 t)$. On the other hand, the EoS parameter can be used to distinguish the phantom and non-phantom dynamics of the Universe. The EoS parameters for the phantom and non-phantom cases are, respectively, given as $w < -1$ and $w \geq -1$. Additionally, the EoS parameter takes $w \approx 0$ in the matter dominant phase, while it takes $w = 1/3$ in the radiation dominant phase.

The time-dependent behavior of the EoS parameter is given in Fig. 6(a). However, the EoS parameter is given by log-log and semi-log scale in Figs. 6(b) and (c), respectively. We note that log-log and semi-log figures are plotted for the absolute value of the EoS parameter after first peaks f_c to obtain the slope of curves. Therefore in Figs. 6(b) and (c), curves are given inversely.

The EoS curves also reflect the transition in scale factor a around t_c in Fig. 6(a). In addition to the deceleration parameter q, the EoS parameter w also has the first initial peak which indicates a sudden acceleration in the time evolution of expansion of the Universe. EoS parameter decays with time according to a power-law $w \propto (t/t_0)^{-\tilde{\eta}}$ up to critical time point t_c as seen in Fig. 6(b). Finally, after a local minimum value, as seen in Fig. 6(c) it again exponentially increases as $w \propto e^{\tilde{\eta}'(t/t_0)}$ up to a current constant value $w = -1$ of the ΛCDM model, as seen in Fig. 6(a)

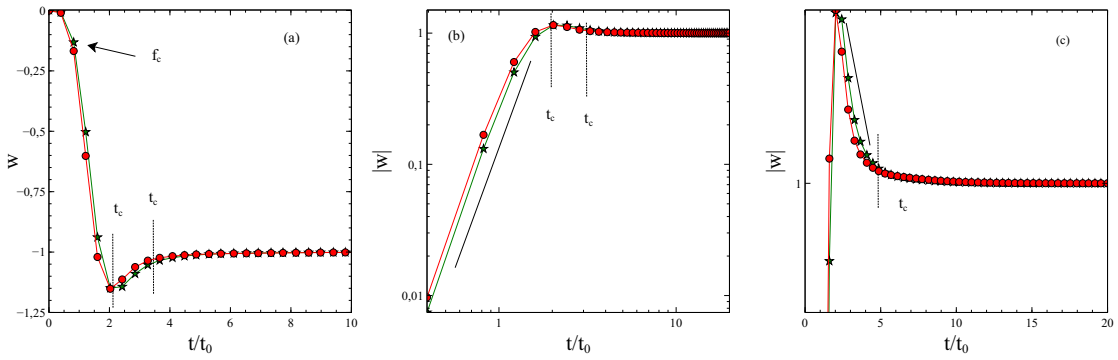

FIG. 6. The EoS parameter $w(t)$ with respect to cosmic time. Here we set the parameter values $\Lambda_1 = 0.05$, $\Lambda_2 = 2.5$, $\Lambda_3 = 0.5$, $\Lambda_4 = 2.05$, $A_1 = A_4 = 1.05$, $A_2 = A_3 = 1.5$, $k_1 = -1.0$, $k_2 = 1.0$ for the red circle line; $\Lambda_1 = 0.1$, $\Lambda_2 = 2.6$, $\Lambda_3 = 0.6$, $\Lambda_4 = 2.2$, $A_1 = A_4 = 1.15$, $A_2 = A_3 = 1.6$, $k_1 = -1.05$, $k_2 = 1.0$ for the green star line is given. In (b), EoS parameter w in Log-Log scale. In (c), EoS parameter w in semi-log plot is shown.

where $\tilde{\eta}$, and $\tilde{\eta}'$ denote arbitrary constant parameters.

In summary, all figures in presented study are plotted by using parameters which satisfy the Hamiltonian constraints present zero energy condition. Obtained numerical results are consistent with observational cosmology and strongly provides our interacting model explain some outstanding problem of the physical cosmology.

VI. THE COSMOLOGICAL PARAMETERS IN THE LIMITING CASES

We obtained the scale factor in terms of equations of motion by solving the FLRW equation with two scalar fields, and then we plotted both the scale factor and other quantities by solving numerically. We see that scale factor can be given in the single formula by

$$a = a_0 (t/t_0)^{2/3} e^{h(t/t_0)}, \tag{29}$$

where a_0 is the normalization constant. Now we can derive other quantities due to scale factor a. The cosmological parameters including Hubble parameter, deceleration, jerk and EoS parameter are respectively given by

$$h = \frac{\dot{a}}{a} = \frac{2}{3}(t/t_0)^{-1} + h_0, \tag{30a}$$

$$q = -\frac{\ddot{a}}{ah^2} = -1 + \frac{6}{(2+3ht/t_0)^2}, \tag{30b}$$

$$j = \frac{\dddot{a}}{ah^3} = 1 + \frac{36}{(2+3ht/t_0)^3} + \frac{18}{(2+3ht/t_0)^2}, \tag{30c}$$

$$w = -\frac{1}{3} - \frac{2a\ddot{a}}{3\dot{a}^2} = -1 + \frac{4}{(2+3ht/t_0)^2} \ . \tag{30d}$$

where h_0 is a constant. It is clear that one obviously obtains power-law and exponential law expansion from Eq. (29) in the limiting cases. Accordingly, for $t/t_0 \to 0$, i.e. $t/t_0 \leq t_c$, the cosmological parameters approximate to the following:

$$a = a_0 (t/t_0)^{2/3},\ h \sim \frac{2}{3}(t/t_0)^{-1},\ q \sim 1/2,\ j \sim 1\ w \sim 0\ . \tag{31}$$

Similarly, the exponential term dominates at late times, such that in the limit $t/t_0 \to \infty$, i.e. $t/t_0 > t_c$, we have

$$a = a_0 e^{ht/t_0},\ h \to h_0,\ q \to -1,\ j \to 1,\ w \to -1 \tag{32}$$

Notice that our results are consistent with the theoretical predictions and observational data in the limiting cases.

VII. DISCUSSION AND CONCLUDING REMARKS

In the introduction, we mentioned that the late time crossover between a power-law to an exponential expansion of the Universe evolution was the leading problem awaiting a recipe in physical cosmology. In this critical regime, the Universe suddenly passes from a matter-dominated era to a dark energy-dominated era. These different eras are characterized by $a(t) \propto (t/t_0)^{\alpha}$ and $a(t) \propto e^{h(t/t_0)}$, respectively.

We know that dark energy is responsible for the late-time exponential expansion of the Universe although we have not known its physical origin. However, the existence of dark energy alone does not seem to be sufficient to explain this catastrophic-like transition. Therefore, in this study, to explain this unexpected and catastrophic-like transition, we propose a dark matter and dark energy interaction model where are represented by a two-scalar fields in a Lagrangian in the framework of the FLRW metric. In our model, two scalar fields interact with a potential which is determined by two oscillators and two anti-oscillators.

We analytically solve the field equations in the FLRW framework for this model and obtain an exact form of the scale factor. We numerically analyse the scale factor and give in Fig. 2. We show that our numerical result produces a hybrid scale factor incorporating the power and exponential terms as $a(t) = a_0(t/t_0)^{\alpha}e^{ht/t_0}$. This main and significant result clearly denotes that there is a crossover at t_c. Below $t/t_0 \leq t_c$, the evolution of the Universe is dominated by matter with $a(t) \propto (t/t_0)^{\alpha}$, on the other hand, above $t/t_0 > t_c$, the evolution is dominated by dark energy with $a \propto \exp(ht/t_0)$. Furthermore, surprisingly, we find that the scale factor behaves as $a \propto (t/t_0)^{2/3}$ below $t/t_0 \leq t_c$, and as $a \propto e^{h(t/t_0)}$ with in the interval of the around $H_0 = 69.5$ and $H_0 = 73.5$ km s^{-1}Mpc^{-1} depend on the weak and strong interactions between dark components above $t/t_0 > t_c$, respectively. The exponent $\alpha = 2/3$ and transition point $t_0 \simeq 9.8$ Gyear in the cosmic time are completely consistent exact solution of the FLRW and observations [54]. It is very consistent with the theoretical solutions [55] and time-dependent Hubble parameter H_0 takes value in the observable intervals given by CMB with Planck [56–58], CMB without Planck [59–61], No CMB, with BBN [62–64], Cepheids-SNIa [65–74], TRGB-SNIa [78–83], Masers [84], Tully-Fisher Relation [85, 86], Surface Brightness Fluctuations [87], Lensing related, mass model-dependent [88–95], Optimistic average [96] and Ultra conservative, no Cepheids, no lensing [97] (For more references please see Ref. [75]).

Furthermore, to see general character and discuss, we numerically obtain other dimensionless quantities such as little Hubble h, deceleration q, jerk parameter j and EoS w by using scale factor a in Figs. 3, 4, 5 and 6, respectively. These parameters reflect different aspects of all information on the scale factor since they are obtained depending on the scale factor and/or its derivatives. Indeed, as one can notice from the relevant descriptions of figures leading to the crossover, late time transition from power-law to the exponential one are obtained. All obtained numerical results are consistent with the observational data and theoretical studies.

We mentioned in the introduction section that dark energy alone may not explain the sudden transition from power-law to the exponential expansion. Based on our finding, we conclude that two coupled scalar and interacting fields corresponding to dark matter and dark energy, respectively, offer a good mechanism to explain this late time turnover behavior. On the other hand, we notice that the chosen potential does not have a catastrophic character and does not directly lead to catastrophic dynamics. The catastrophic potentials are very special types and an extensive classification has been given by Thom in Ref. [22]. Here, to find an exact solution, we linearized the potential in Eq. (7) by Taylor series expansion. One can see from Eq. (13) that the potential, including higher-order terms, has polynomial characters. Thus, our interaction potential is approximately fitting to any catastrophic potential. It serves to establish a relation between the sudden transition and the interaction potential.

Additionally, our study also draws attention to the importance of the cosmology models with scalar fields. In fact, in the previous work [53] it was shown that the classical models of gravitation interacting with scalar fields may exhibit transitions between different domains. Similarly, we obtain a transition in the same theoretical framework with help of interacting potential mentioned this presented study. Therefore, we conclude scalar field cosmology models deserve attention.

In summary, we consider the interaction of two scalar fields corresponding to dark matter and dark energy in the FRLW framework. We show by using this interacting model that the late time observational crossover of the Universe can be explained. We present a hybrid scale factor formula which is directly obtained from our model itself. Our solutions are consistent with the matter dominated era and dark energy dominated era. Furthermore, we show that the dark matter and dark energy interactions can provide a novel mechanism to explain the catastrophic-like transition in the time evolution of the Universe as well for cosmic coincidence and singularity. Finally, we emphasize that the model, at the same time, also provides information about the interaction mechanism of dark matter and dark energy in the model universe. On the other hand, the method we use here can be generalized to the many scalar fields interacting linearly or non-linearly to discuss the open problems of the cosmology and apply the Chaotic Universe Theory in Ref.[28] to obtain the metric dependent solutions.

ACKNOWLEDGEMENTS

The author Isil Basaran-Öz grateful to Istanbul University for hospitality and grant for the Post-Doctoral Researcher Position at Istanbul University. This work was supported by Istanbul University Post-Doctoral Research Project: MAB-2019-33386 which is titled "The metric dependent investigation of Chaotic Universe Theory".

AUTHOR CONTRIBUTIONS STATEMENT

E. A. and T. D. developed the theory. All co-authors performed to obtain the analytical solutions. E. A. and I. B.-O. obtained the numerical results and plotted figures. E. A and T. D. interpreted the results. E. A. wrote the manuscript and revised the last version of the manuscript.

---

[1] A. G. Riess, A. V. Filippenko, P. Challis, A. Clocchiatti, A. Diercks, P. M. Garnavich, R. L. Gilliland, C. J. Hogan, S. Jha, R. P. Kirshner, B. Leibundgut, M. M. Phillips, D. Reiss, B. P. Schmidt, R. A. Schommer, R. C. Smith, J. Spyromilio, C. Stubbs, N. B. Suntzeff, and J. Tonry, Observational evidence from supernovae for an accelerating universe and a cosmological constant, The Astronomical Journal **116**, 1009 (1998), astro-ph/9805201.

[2] S. Perlmutter, G. Aldering, G. Goldhaber, R. A. Knop, P. Nugent, P. G. Castro, S. Deustua, S. Fabbro, A. Goobar, D. E. Groom, I. M. Hook, A. G. Kim, M. Y. Kim, J. C. Lee, N. J. Nunes, R. Pain, C. R. Pennypacker, R. Quimby, C. Lidman, R. S. Ellis, M. Irwin, R. G. McMahon, P. Ruiz-Lapuente, N. Walton, B. Schaefer, B. J. Boyle, A. V. Filippenko, T. Matheson, A. S. Fruchter, N. Panagia, H. J. M. Newberg, W. J. Couch, and T. S. C. Project, Measurements of ω and λ from 42 high redshift supernovae, The Astrophysical Journal **517**, 565 (1999).

[3] A. D. Linde, A new inflationary universe scenario: A possible solution of the horizon, flatness, homogeneity, isotropy and primordial monopole problems, Physics Letters B **108**, 389 (1982).

[4] S. Weinberg, *Cosmology* (Oxford University Press, USA, 2008).

[5] T. Barreiro, E. J. Copeland, and N. J. Nunes, Quintessence arising from exponential potentials, Phys. Rev. D **61**, 127301 (2000), arXiv:astro-ph/9910214.

[6] R. R. Caldwell, A phantom menace? cosmological consequences of a dark energy component with super-negative equation of state, Physics Letters B **545**, 23 (2002), arXiv:astro-ph/9908168.

[7] C. Armendariz-Picon, V. Mukhanov, and P. J. Steinhardt, Essentials of k-essence, Phys. Rev. D **63**, 103510 (2001), arXiv:astro-ph/0006373.

[8] J. S. Bagla, H. K. Jassal, and T. Padmanabhan, Cosmology with tachyon field as dark energy, Phys. Rev. D **67**, 063504 (2003), arXiv:astro-ph/0212198.

[9] M. C. Bento, O. Bertolami, and A. A. Sen, Generalized chaplygin gas, accelerated expansion, and dark-energy-matter unification, Phys. Rev. D **66**, 043507 (2002), arXiv:gr-qc/0202064.

[10] M. Li, A model of holographic dark energy, Physics Letters B **603**, 1 (2004), arXiv:hep-th/0403127.

[11] S. Capozziello and M. Roshan, Exact cosmological solutions from hojman conservation quantities, Phys. Lett. B **726**, 471 (2013), arXiv:1308.3910 [gr-qc].

[12] J. A. Belinchón, T. Harko, and M. K. Mak, Exact scalar–tensor cosmological models, Int. J. Mod. Phys. D **26**, 1750073 (2017), arXiv:1612.05446 [gr-qc].

[13] B. Tajahmad, Studying the intervention of an unusual term in $f(t)$ gravity via the noether symmetry approach, Eur. Phys. J. C **77**, 510 (2017), arXiv:1701.01620 [gr-qc].

[14] M. Sharif and I. Nawazish, Cosmological analysis of scalar field models in $f(r,t)$ gravity, Eur. Phys. J. C **77**, 198 (2017), arXiv:1703.06763 [gr-qc].

[15] A. Paliathanasis and G. Leon, Analytic solutions in einstein-aether scalar field cosmology, Eur. Phys. J. C **80**, 355 (2020), arXiv:2003.03903 [gr-qc].

[16] A. Paliathanasis and M. Tsamparlis, Two scalar field cosmology: Conservation laws and exact solutions, Phys. Rev. D **90**, 043529 (2014), arXiv:1408.1798 [gr-qc].

[17] Y. Kucukakca and A. R. Akbarieh, Noether symmetries of einstein-aether scalar field cosmology, Eur. Phys. J. C **80**, 1019 (2020).

[18] S. Nojiri, S. Odintsov, and V. Oikonomou, Modified gravity theories on a nutshell: Inflation, bounce and late-time evolution, Physics Reports **692**, 1 (2017), modified Gravity Theories on a Nutshell: Inflation, Bounce and Late-time Evolution.

[19] S. Nojiri and S. Odintsov, Unifying phantom inflation with late-time acceleration: scalar phantom–non-phantom transition model and generalized holographic dark energy, General Relativity and Gravitation **38**, 1572 (2006).

[20] I. Oz, Y. Kucukakca, and N.Unal, Anisotropic solution in phantom cosmology via noether symmetry approach1, Can. J. Phys. **96**, 677 (2018).

[21] S. Bahamonde, C. G. Böhmer, S. Carloni, E. J. Copeland, W. Fang, and N. Tamanini, Dynamical systems applied to cosmology: Dark energy and modified gravity, Physics Reports **775-777**, 1 (2018).

[22] R. Thom, *Structural Stability and Morphogenesis: An Outline of a General Theory of Models*, Advanced book classics (CRC Press, Taylor & Francis GroupPerseus Books, 1989).

[23] R. R. Caldwell, R. Dave, and P. J. Steinhardt, Cosmological imprint of an energy component with general equation of state, Phys. Rev. Lett. **80**, 1582 (1998), arXiv:astro-ph/9708069.

[24] A. R. Liddle and R. J. Scherrer, Classification of scalar field potentials with cosmological scaling solutions, Phys. Rev. D **59**, 023509 (1998), arXiv:astro-ph/9809272.

[25] P. Peebles and B. Ratra, The cosmological constant and dark energy, Rev. Mod. Phys. **75**, 559 (2003), arXiv:astro-ph/0207347.

[26] C. Wetterich, Cosmology and the fate of dilatation symmetry, Nuclear Physics B **302**, 668 (1988), arXiv:1711.03844 [hep-th].

[27] J. D. Barrow, Quiescent cosmology, Nature **272**, 211 (1978).

[28] E. Aydiner, Chaotic universe model, Scientific Reports **8**, 721 (2018).

[29] P. Brax and J. Martin, The supergravity quintessence model coupled to the minimal supersymmetric standard model, Journal of Cosmology and Astroparticle Physics **11**, 008, arXiv:astro-ph/0606306.

[30] Y. L. Bolotin, A. Kostenko, O. Lemets, and D. Yerokhin, Cosmological evolution with interaction between dark energy and dark matter, International Journal of Modern Physics D **24**, 1530007 (2015), arXiv:1310.0085 [astro-ph.CO].

[31] W. Zimdahl and D. Pavon, Statefinder parameters for interacting dark energy, General Relativity and Gravitation **36**, 1483–1491 (2004), arXiv:gr-qc/0311067.

[32] L. Amendola, G. C. Campos, and R. Rosenfeld, Consequences of dark matter-dark energy interaction on cosmological parameters derived from type ia supernova data, Phys. Rev. D **75**, 083506 (2007), arXiv:astro-ph/0610806.

[33] B. Wang, E. Abdalla, F. Atrio-Barandela, and D. Pavon, Dark matter and dark energy interactions: theoretical challenges, cosmological implications and observational signatures, Reports on Progress in Physics **79**, 096901 (2016), arXiv:1603.08299 [astro-ph.CO].

[34] C. G. Böhmer, N. Tamanini, and M. Wright, Interacting quintessence from a variational approach. i. algebraic couplings, Phys. Rev. D **91**, 123002 (2015), arXiv:1501.06540 [gr-qc].

[35] C. G. Böhmer, N. Tamanini, and M. Wright, Interacting quintessence from a variational approach. ii. derivative couplings, Phys. Rev. D **91**, 123003 (2015), arXiv:1502.04030 [gr-qc].

[36] J.-H. He and B. Wang, Effects of the interaction between dark energy and dark matter on cosmological parameters, Journal of Cosmology and Astroparticle Physics **06**, 010, arXiv:70801.4233 [astro-ph].

[37] R.-G. Cai, N. Tamanini, and T. Yang, Reconstructing the dark sector interaction with LISA, Journal of Cosmology and Astroparticle Physics **05**, 031, arXiv:1703.07323 [astro-ph.CO].

[38] W. Yang, N. Banerjee, A. Paliathanasis, and S. Pan, Reconstructing the dark matter and dark energy interaction scenarios from observations, Physics of the Dark Universe **26**, 100383 (2019), arXiv:1812.06854 [astro-ph.CO].

[39] L. Amendola, Coupled quintessence, Phys. Rev. D **62**, 043511 (2000), arXiv:astro-ph/9908023.

[40] D. Tocchini-Valentini and L. Amendola, Stationary dark energy with a baryon-dominated era: Solving the coincidence problem with a linear coupling, Phys. Rev. D **65**, 063508 (2002), arXiv:astro-ph/0108143.

[41] L. Amendola and C. Quercellini, Tracking and coupled dark energy as seen by the wilkinson microwave anisotropy probe, Phys. Rev. D **68**, 023514 (2003), arXiv:astro-ph/0303228.

[42] S. del Campo, R. Herrera, and D. Pavon, Toward a solution of the coincidence problem, Phys. Rev. D **78**, 021302 (2008), arXiv:0806.2116 [astro-ph].

[43] S. del Campo, R. Herrera, and D. Pavon, Interacting models may be key to solve the cosmic coincidence problem, Journal of Cosmology and Astroparticle Physics (01), 020, arXiv:0812.2210 [gr-qc].

[44] H. Wei and S. N. Zhang, Observational h(z) data and cosmological models, Physics Letters B **644**, 7 (2007), arXiv:astro-ph/0609597.

[45] S. del Campo, R. Herrera, and D. Pavón, Interaction in the dark sector, Phys. Rev. D **91**, 123539 (2015), arXiv:1507.00187 [gr-qc].

[46] L. P. Chimento, Linear and nonlinear interactions in the dark sector, Phys. Rev. D **81**, 043525 (2010), arXiv:0911.5687 [astro-ph.CO].

[47] G. Sanchez and E. Ivan, Dark matter interacts with variable vacuum energy, Gen. Rel. Grav. **46**, 1769 (2014), arXiv:1405.1291 [gr-qc].

[48] M. M. Verma, Dark energy as a manifestation of the non-constant cosmological constant, Astrophys Space Sci **330**, 101 (2010).

[49] M. Shahalam, S. D. Pathak, M. M. Verma, M. Y. Khlopov, and R. Myrzakulov, Dynamics of interacting quintessence, Eur. Phys. J. C **75**, 395 (2015), arXiv:1503.08712 [gr-qc].

[50] M. Cruz and S. Lepe, Holographic approach for dark energy–dark matter interaction in curved FLRW spacetime, Classical and Quantum Gravity **35**, 155013 (2018).

[51] M. Cruz, S. Lepe, and G. Morales-Navarrete, Qualitative description of the universe in the interacting fluids scheme, Nuclear Physics B **943**, 114623 (2019).

[52] R. Saleem and M. J. Imtiaz, Dynamical study of interacting ricci dark energy model using chevallier-polarsky-lindertype parametrization, Classical and Quantum Gravity **37**, 065018 (2020).

[53] T. Dereli and R. W. Tucker, Signature dynamics in general relativity, Classical and Quantum Gravity **10**, 365 (1993).

[54] B. Ryden, *Introduction to cosmology*, 2nd ed. (Cambridge University Press, New York, NY, 2016).

[55] A. Einstein and W. de Sitter, On the relation between the expansion and the mean density of the universe, Proceedings of the National Academy of Sciences **18**, 213 (1932), https://www.pnas.org/content/18/3/213.full.pdf.

[56] L. Balkenhol *et al.* (SPT), Constraints on ΛCDM Extensions from the SPT-3G 2018 EE and TE Power Spectra, (2021), arXiv:2103.13618 [astro-ph.CO].

[57] N. Aghanim *et al.* (Planck), Planck 2018 results. VI. Cosmological parameters, Astron. Astrophys. **641**, A6 (2020), arXiv:1807.06209 [astro-ph.CO].

[58] N. Aghanim *et al.* (Planck), Planck 2018 results. V. CMB power spectra and likelihoods, Astron. Astrophys. **641**, A5 (2020), arXiv:1907.12875 [astro-ph.CO].

[59] D. Dutcher *et al.* (SPT-3G), Measurements of the E-Mode Polarization and Temperature-E-Mode Correlation of the CMB from SPT-3G 2018 Data, (2021), arXiv:2101.01684 [astro-ph.CO].

[60] S. Aiola *et al.* (ACT), The Atacama Cosmology Telescope: DR4 Maps and Cosmological Parameters, JCAP **12**, 047, arXiv:2007.07288 [astro-ph.CO].

[61] X. Zhang and Q.-G. Huang, Constraints on H_0 from WMAP and BAO Measurements, Commun. Theor. Phys. **71**, 826 (2019), arXiv:1812.01877 [astro-ph.CO].

[62] O. H. E. Philcox, M. M. Ivanov, M. Simonović, and M. Zaldarriaga, Combining Full-Shape and BAO Analyses of Galaxy Power Spectra: A 1.6\% CMB-independent constraint on H_0, JCAP **05**, 032, arXiv:2002.04035 [astro-ph.CO].

[63] M. M. Ivanov, M. Simonović, and M. Zaldarriaga, Cosmological Parameters from the BOSS Galaxy Power Spectrum, JCAP **05**, 042, arXiv:1909.05277 [astro-ph.CO].

[64] S. Alam *et al.* (eBOSS), Completed SDSS-IV extended Baryon Oscillation Spectroscopic Survey: Cosmological implications from two decades of spectroscopic surveys at the Apache Point Observatory, Phys. Rev. D **103**, 083533 (2021), arXiv:2007.08991 [astro-ph.CO].

[65] A. G. Riess, S. Casertano, W. Yuan, J. B. Bowers, L. Macri, J. C. Zinn, and D. Scolnic, Cosmic Distances Calibrated to 1% Precision with Gaia EDR3 Parallaxes and Hubble Space Telescope Photometry of 75 Milky Way Cepheids Confirm Tension with ΛCDM, Astrophys. J. Lett. **908**, L6 (2021), arXiv:2012.08534 [astro-ph.CO].

[66] L. Breuval *et al.*, The Milky Way Cepheid Leavitt law based on Gaia DR2 parallaxes of companion stars and host open cluster populations, Astron. Astrophys. **643**, A115 (2020), arXiv:2006.08763 [astro-ph.SR].

[67] A. G. Riess, S. Casertano, W. Yuan, L. M. Macri, and D. Scolnic, Large Magellanic Cloud Cepheid Standards Provide a 1% Foundation for the Determination of the Hubble Constant and Stronger Evidence for Physics beyond ΛCDM, Astrophys. J. **876**, 85 (2019), arXiv:1903.07603 [astro-ph.CO].

[68] D. Camarena and V. Marra, Local determination of the Hubble constant and the deceleration parameter, Phys. Rev. Res. **2**, 013028 (2020), arXiv:1906.11814 [astro-ph.CO].

[69] C. R. Burns *et al.* (CSP), The Carnegie Supernova Project: Absolute Calibration and the Hubble Constant, Astrophys. J. **869**, 56 (2018), arXiv:1809.06381 [astro-ph.CO].

[70] B. Follin and L. Knox, Insensitivity of the distance ladder Hubble constant determination to Cepheid calibration modelling choices, Mon. Not. Roy. Astron. Soc. **477**, 4534 (2018), arXiv:1707.01175 [astro-ph.CO].

[71] S. M. Feeney, D. J. Mortlock, and N. Dalmasso, Clarifying the Hubble constant tension with a Bayesian hierarchical model of the local distance ladder, Mon. Not. Roy. Astron. Soc. **476**, 3861 (2018), arXiv:1707.00007 [astro-ph.CO].

[72] A. G. Riess *et al.*, A 2.4% Determination of the Local Value of the Hubble Constant, Astrophys. J. **826**, 56 (2016), arXiv:1604.01424 [astro-ph.CO].

[73] W. Cardona, M. Kunz, and V. Pettorino, Determining H_0 with Bayesian hyper-parameters, JCAP **03**, 056, arXiv:1611.06088 [astro-ph.CO].

[74] W. L. Freedman, B. F. Madore, V. Scowcroft, C. Burns, A. Monson, S. E. Persson, M. Seibert, and J. Rigby, Carnegie Hubble Program: A Mid-Infrared Calibration of the Hubble Constant, Astrophys. J. **758**, 24 (2012), arXiv:1208.3281 [astro-ph.CO].

[75] E. Di Valentino, O. Mena, S. Pan, L. Visinelli, W. Yang, A. Melchiorri, D. F. Mota, A. G. Riess, and J. Silk, In the Realm of the Hubble tension − a Review of Solutions 10.1088/1361-6382/ac086d (2021), arXiv:2103.01183 [astro-ph.CO].

[76] A. G. Riess, L. Macri, S. Casertano, M. Sosey, H. Lampeitl, H. C. Ferguson, A. V. Filippenko, S. W. Jha, W. Li, R. Chornock, and D. Sarkar, A redetermination of the hubble constant with the hubble space telescope from a differerntiaı distance ladder, The Astrophysical Journal **699**, 539 (2009).

[77] Damn you, little h! (or, real-world applications of the hubble constant using observed and simulated data), .

[78] J. Soltis, S. Casertano, and A. G. Riess, The Parallax of ω Centauri Measured from Gaia EDR3 and a Direct, Geometric Calibration of the Tip of the Red Giant Branch and the Hubble Constant, Astrophys. J. Lett. **908**, L5 (2021), arXiv:2012.09196 [astro-ph.GA].

[79] W. L. Freedman, B. F. Madore, T. Hoyt, I. S. Jang, R. Beaton, M. G. Lee, A. Monson, J. Neeley, and J. Rich, Calibration of the Tip of the Red Giant Branch (TRGB) 10.3847/1538-4357/ab7339 (2020), arXiv:2002.01550 [astro-ph.GA].

[80] M. J. Reid, D. W. Pesce, and A. G. Riess, An Improved Distance to NGC 4258 and its Implications for the Hubble Constant, Astrophys. J. Lett. **886**, L27 (2019), arXiv:1908.05625 [astro-ph.GA].

[81] W. L. Freedman *et al.*, The Carnegie-Chicago Hubble Program. VIII. An Independent Determination of the Hubble Constant Based on the Tip of the Red Giant Branch 10.3847/1538-4357/ab2f73 (2019), arXiv:1907.05922 [astro-ph.CO].

[82] W. Yuan, A. G. Riess, L. M. Macri, S. Casertano, and D. Scolnic, Consistent Calibration of the Tip of the Red Giant Branch in the Large Magellanic Cloud on the Hubble Space Telescope Photometric System and a Re-determination of the Hubble Constant, Astrophys. J. **886**, 61 (2019), arXiv:1908.00993 [astro-ph.GA].

[83] I. S. Jang and M. G. Lee, The Tip of the Red Giant Branch Distances to Typa Ia Supernova Host Galaxies. V. NGC 3021, NGC 3370, and NGC 1309 and the Value of the Hubble Constant, Astrophys. J. **836**, 74 (2017), arXiv:1702.01118 [astro-ph.CO].

[84] D. W. Pesce *et al.*, The Megamaser Cosmology Project. XIII. Combined Hubble constant constraints, Astrophys. J. Lett. **891**, L1 (2020), arXiv:2001.09213 [astro-ph.CO].

[85] E. Kourkchi, R. B. Tully, G. S. Anand, H. M. Courtois, A. Dupuy, J. D. Neill, L. Rizzi, and M. Seibert, Cosmicflows-4: The Calibration of Optical and Infrared Tully–Fisher Relations, Astrophys. J. **896**, 3 (2020), arXiv:2004.14499 [astro-ph.GA].

[86] J. Schombert, S. McGaugh, and F. Lelli, Using the Baryonic Tully–Fisher Relation to Measure H o, Astron. J. **160**, 71 (2020), arXiv:2006.08615 [astro-ph.CO].

[87] J. P. Blakeslee, J. B. Jensen, C.-P. Ma, P. A. Milne, and J. E. Greene, The Hubble Constant from Infrared Surface Brightness Fluctuation Distances, Astrophys. J. **911**, 65 (2021), arXiv:2101.02221 [astro-ph.CO].

[88] M. Millon *et al.*, TDCOSMO. I. An exploration of systematic uncertainties in the inference of H_0 from time-delay cosmography, Astron. Astrophys. **639**, A101 (2020), arXiv:1912.08027 [astro-ph.CO].

[89] J.-Z. Qi, J.-W. Zhao, S. Cao, M. Biesiada, and Y. Liu, Measurements of the Hubble constant and cosmic curvature with quasars: ultracompact radio structure and strong gravitational lensing, Mon. Not. Roy. Astron. Soc. **503**, 2179 (2021), arXiv:2011.00713 [astro-ph.CO].

[90] K. Liao, A. Shafieloo, R. E. Keeley, and E. V. Linder, Determining Model-independent H 0 and Consistency Tests, Astrophys. J. Lett. **895**, L29 (2020), arXiv:2002.10605 [astro-ph.CO].

[91] K. Liao, A. Shafieloo, R. E. Keeley, and E. V. Linder, A model-independent determination of the Hubble constant from lensed quasars and supernovae using Gaussian process regression, Astrophys. J. Lett. **886**, L23 (2019), arXiv:1908.04967 [astro-ph.CO].

[92] A. J. Shajib *et al.* (DES), STRIDES: a 3.9 per cent measurement of the Hubble constant from the strong lens system DES J0408−5354, Mon. Not. Roy. Astron. Soc. **494**, 6072 (2020), arXiv:1910.06306 [astro-ph.CO].

[93] K. C. Wong *et al.*, H0LiCOW – XIII. A 2.4 per cent measurement of H0 from lensed quasars: 5.3σ tension between early- and late-Universe probes, Mon. Not. Roy. Astron. Soc. **498**, 1420 (2020), arXiv:1907.04869 [astro-ph.CO].

[94] S. Birrer *et al.*, H0LiCOW - IX. Cosmographic analysis of the doubly imaged quasar SDSS 1206+4332 and a new measurement of the Hubble constant, Mon. Not. Roy. Astron. Soc. **484**, 4726 (2019), arXiv:1809.01274 [astro-ph.CO].

[95] V. Bonvin *et al.*, H0LiCOW – V. New COSMOGRAIL time delays of HE 0435−1223: H_0 to 3.8 per cent precision from strong lensing in a flat ΛCDM model, Mon. Not. Roy. Astron. Soc. **465**, 4914 (2017), arXiv:1607.01790 [astro-ph.CO].

[96] E. Di Valentino, A. Mukherjee, and A. A. Sen, Dark Energy with Phantom Crossing and the H_0 Tension, Entropy **23**, 404 (2021), arXiv:2005.12587 [astro-ph.CO].

[97] E. Di Valentino, S. Pan, W. Yang, and L. A. Anchordoqui, Touch of neutrinos on the vacuum metamorphosis: Is the H_0 solution back?, Phys. Rev. D **103**, 123527 (2021), arXiv:2102.05641 [astro-ph.CO].

Figures

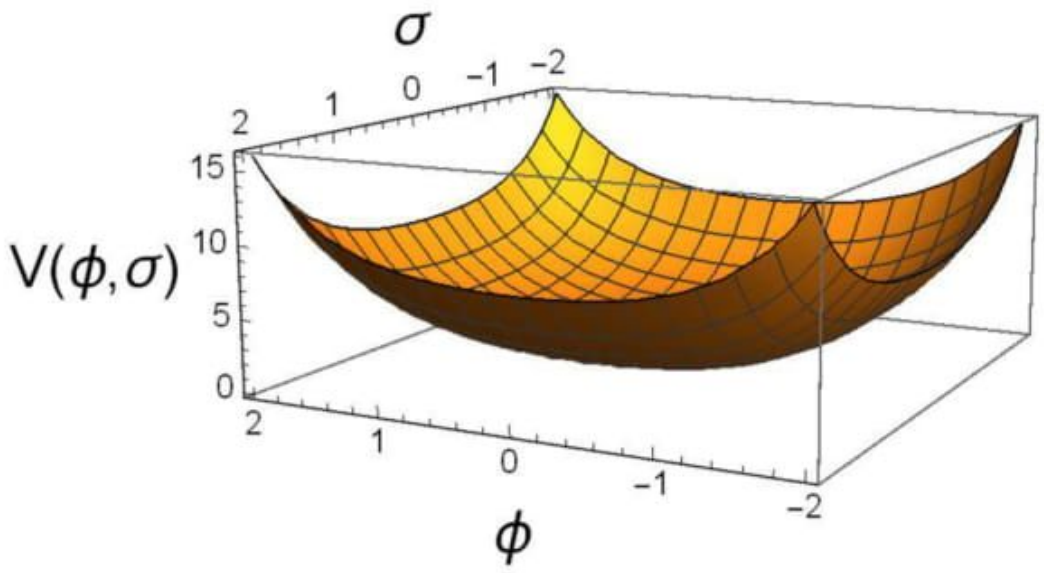

Figure 1

The potential surface of V as a function of field variables and σ . We set values as A1 = B2 = 1.005, A2 = B1 = 2.005, k = 0.005.

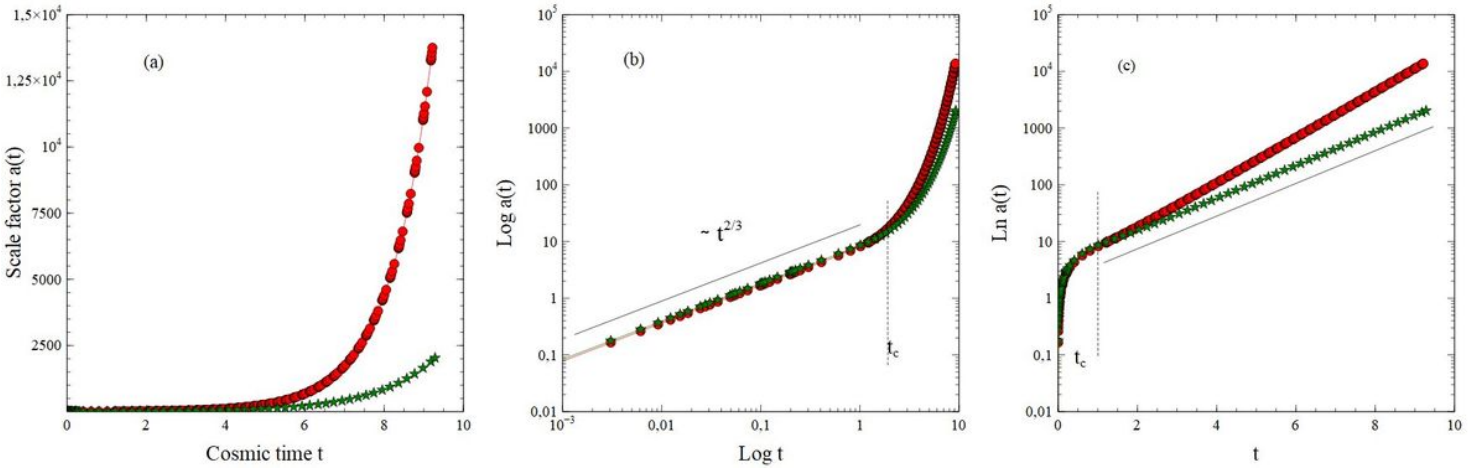

Figure 2

In (a), the scale factor a(t) with respect to the cosmic time is given. Here we set the parameter values A1 = B2 = 1.005, A2 = B1 = 2.005 and k = 0.005 for the red circle line; A1 = B2 = 3.05, A2 = B1 = 3.15 and k = −2.95 for the green star line. In (b), scale factor in Log-Log scale is given. In (c), scale factor a(t) in semi-log plot is displayed. Here tc value is given by Eq. (25).

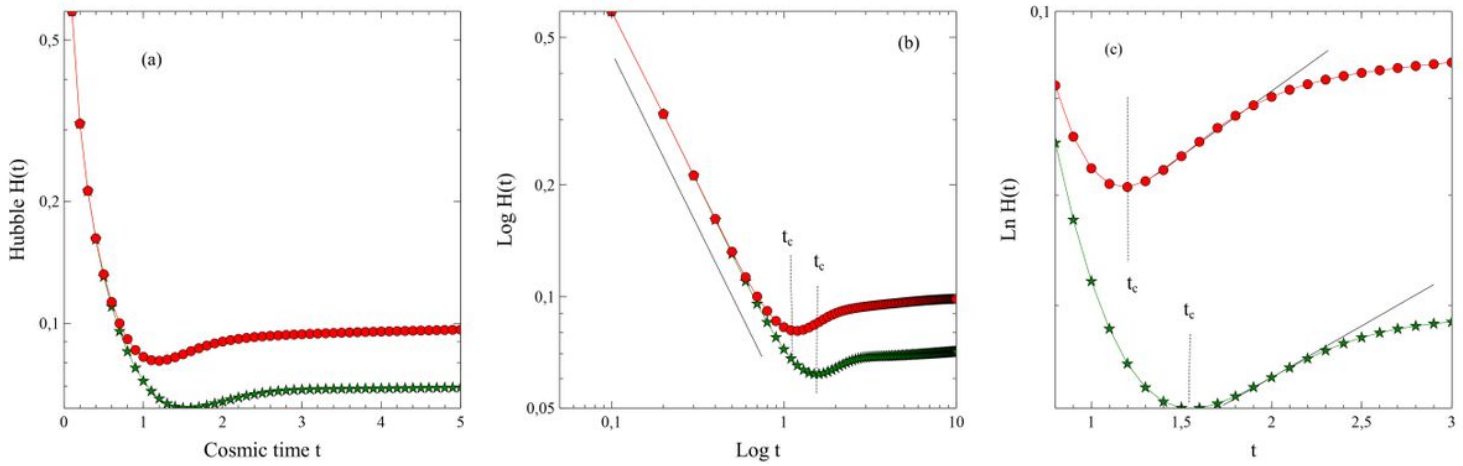

Figure 3

In (a), the Hubble parameter H(t) with respect to cosmic time is given. Here we set the parameter values A1 = B2 = 1.005, A2 = B1 = 2.005 and k = 0.005 for the red circle line; A1 = B2 = 3.05, A2 = B1 = 3.15 and k = −2.95 for the green star line. In (b), Hubble parameter H(t) in Log-Log scale is displayed. In (c), Hubble parameter H(t) in semi-log plot is shown.

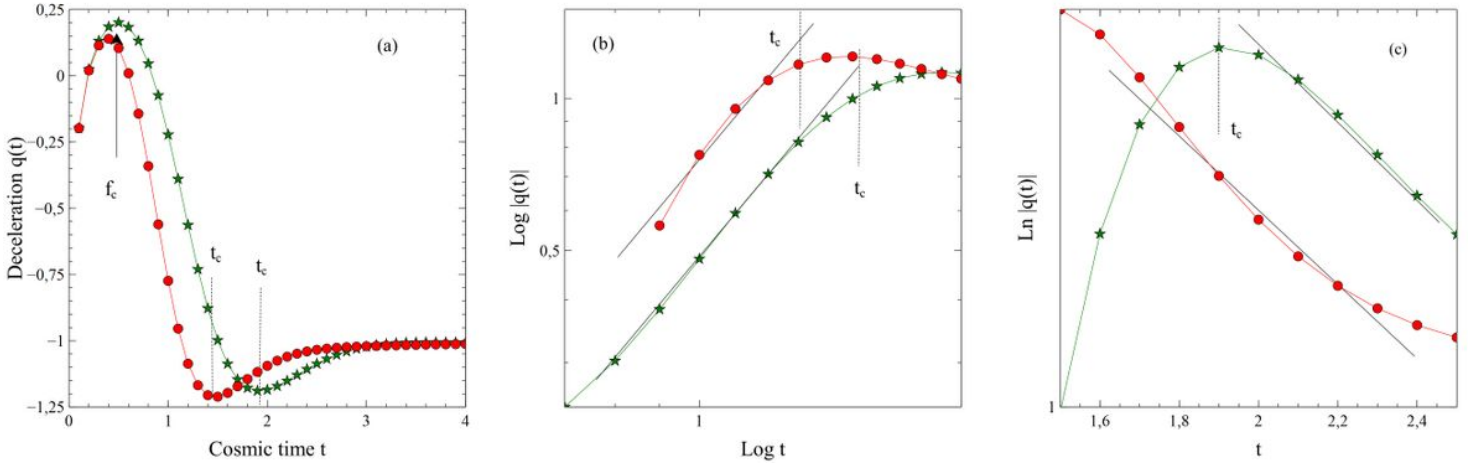

Figure 4

The deceleration parameter q(t) with respect to cosmic time is displayed. Here we set the parameter values A1 = B2 = 1.005, A2 = B1 = 2.005 and k = 0.005 for the red circle line; A1 = B2 = 3.05, A2 = B1 = 3.15 and k = −2.95 for the green star line. In (b), deceleration parameter q(t) in Log-Log scale is shown. In (c), deceleration parameter q(t) in semi-log plot is provided.

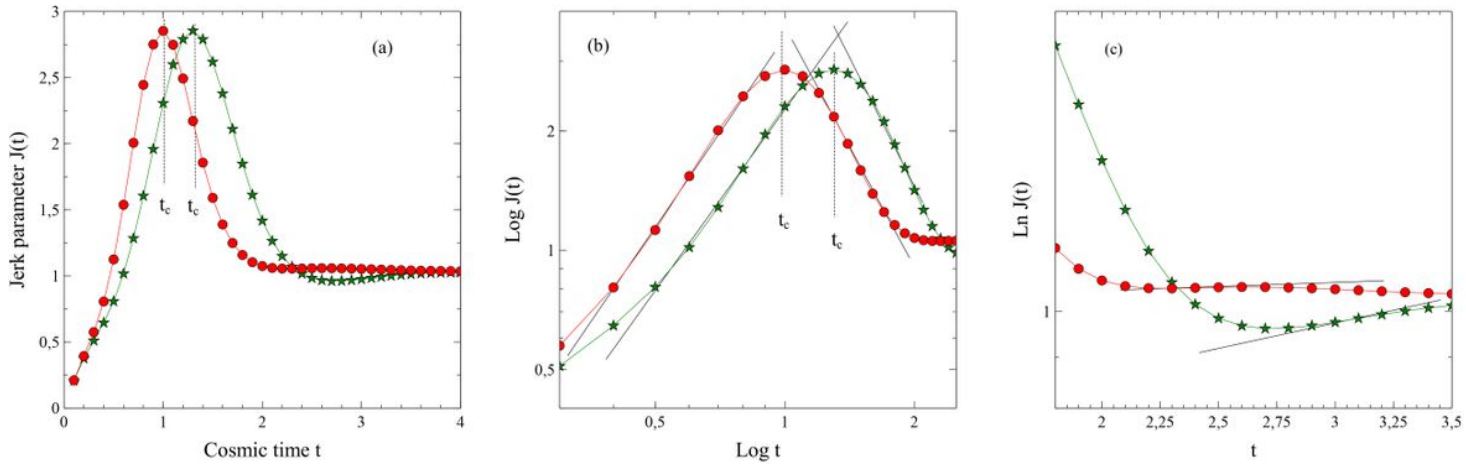

Figure 5

The jerk parameter j(t) with respect to cosmic time. Here we set the parameter values A1 = B2 = 1.005, A2 = B1 = 2.005 and k = 0.005 for the red circle line; A1 = B2 = 3.05, A2 = B1 = 3.15 and k = −2.95 for the green star line. In (b), jerk parameter j(t) in Log-Log scale is provided. In (c), jerk parameter j(t) in semi-log plot is shown.

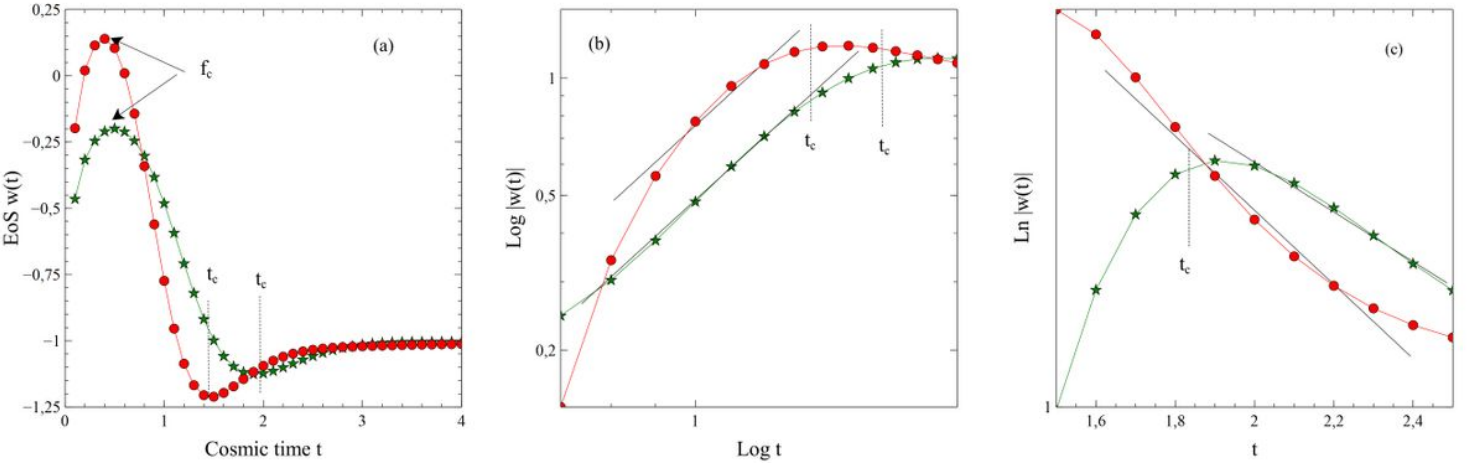

Figure 6

The EoS parameter w(t) with respect to cosmic time. Here we set the parameter values A1 = B2 = 1.005, A2 = B1 = 2.005 and k = 0.005 for the red circle line; A1 = B2 = 3.05, A2 = B1 = 3.15 and k = −2.95 for the green star line is given. In (b), EoS parameter w(t) in Log-Log scale. In (c), EoS parameter w(t) in semi-log plot is shown.